

Article

Structural Characterization of Octahedral Sheet in Dioctahedral Smectites by Thermal Analysis

Xiaoli Wang ^{1,2}, Yan Li ^{1,2} and Hejing Wang ^{1,2,*} 

¹ School of Earth and Space Sciences, Peking University, Beijing 100871, China; xiaoli.wang@pku.edu.cn (X.W.); liyan-pku@163.com (Y.L.)

² Key Laboratory of Orogenic Belt and Crustal Evolution, Ministry of Education, Beijing 100871, China

* Correspondence: hjwang@pku.edu.cn; Tel.: +86-010-6275-0764

Received: 9 March 2020; Accepted: 10 April 2020; Published: 13 April 2020



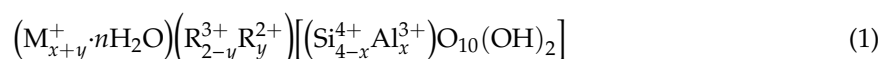
Abstract: The structures of octahedral sheets of dioctahedral phyllosilicates show *cis*-vacant (*cv*) and *trans*-vacant (*tv*) configurations due to the different distributions of the octahedral cations over *cis*- and *trans*-sites. On the basis of the different dehydroxylation temperatures, a thermal analysis is an effective method used to identify the *cv* and *tv* configurations of an octahedral sheet in dioctahedral smectites. The proportions of *cv* and *tv* configurations were determined by fitting the derivative thermogravimetry (DTG) curves. A wide range of *cv* and *tv* proportions were detected in the samples. The dehydroxylation temperatures of samples consisting of *cv* configuration are about 150 to 200 °C higher than those consisting of *tv* configurations. The samples were classified as *tv* varieties when octahedral Fe³⁺ > 0.46 mol/FU, and the pure *tv* dioctahedral smectites were found when Fe³⁺ > 1.8 mol/FU. A clear linear relationship was found between the content of octahedral Fe³⁺ and Al³⁺ and the proportion of *cv* and *tv* configurations. The substitution of Al³⁺ by Fe³⁺ in the octahedral sheets is the main factor for the formation of *tv* varieties. There was no relationship detected between the layer charge density, octahedral Mg²⁺ content, and the proportion of *tv* and *cv*. The present results indicate that the iron content has a significant effect on the structure of the octahedral sheet.

Keywords: *cis*-vacant; *trans*-vacant; dioctahedral smectites; dehydroxylation; thermal analysis

1. Introduction

Smectites are used widely in industrial and environmental applications due to their physical and chemical properties, for example, cation exchange capacity, swelling behavior, and adsorption capacity [1]. The properties of smectites are closely related to their structural features [2,3].

Smectites are typical 2:1 layers of clay minerals, composed of two tetrahedral silicate sheets (T) and one octahedral sheet (O). In each layer, the octahedral sheet is sandwiched between the two tetrahedral sheets (TOT) (Figure 1). In the tetrahedral sheets, the dominant cation is Si⁴⁺, but it can often be substituted by trivalent cation such as Al³⁺. In the octahedral sheet, the common cations are Al³⁺, Mg²⁺, Fe³⁺, or Fe²⁺, but other cations, such as Li⁺, Ni²⁺, and Cr³⁺ have also been identified in octahedral sites. Two arrangements exist in the octahedral sheet, if all octahedral sites are filled with bivalent cations such as Mg²⁺ and Fe²⁺, the structure is called trioctahedral; if two-thirds of octahedral sites are occupied by trivalent cations such as Al³⁺ and Fe³⁺, the structure is known as dioctahedral. The general chemical formula for dioctahedral smectites is:



where M⁺ represents the exchangeable interlayer cations; R²⁺ and R³⁺ refer to divalent and trivalent octahedral cations, respectively; *x* and *y* indicate the tetrahedral and octahedral layer charge,

respectively [2]. The most important species of dioctahedral smectites are montmorillonite, beidellite, and nontronite. In general, octahedra shows two different configurations related to the disposition of hydroxyl groups, for example, *cis*- and *trans*-octahedron. In the *cis*-octahedron, the OH groups are on the same side, whereas in the *trans*-octahedron, the OH groups are on the opposite side (Figure 2).

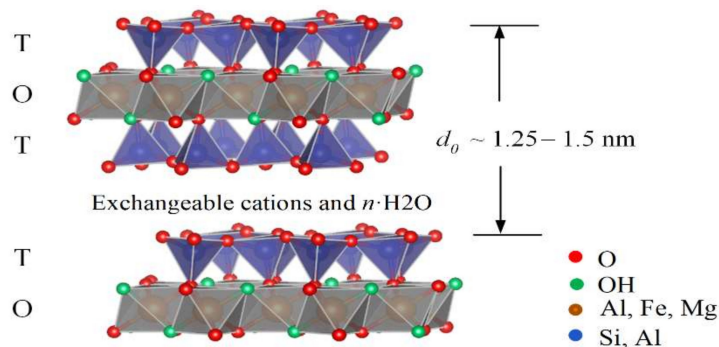


Figure 1. General structure of smectites.

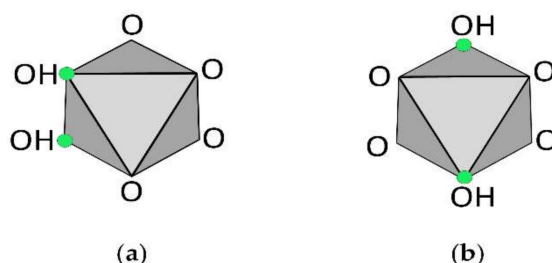


Figure 2. Structure of (a) *cis*-octahedron and (b) *trans*-octahedron.

In dioctahedral smectites, one third of the octahedral positions are vacant. Thus, the octahedral sheet with *cis*-sites vacant is called the *cis*-vacant (*cv*) configuration (Figure 3a), and with *trans*-sites vacant it is called the *trans*-vacant (*tv*) configuration (Figure 3b). This kind of cations' distribution was first proposed by Méring and Oberlin in 1971 [4]. Then, Tsipursky and Drits [5] found that natural dioctahedral smectites cover a wide range of proportions of *cv* and *tv* structures, and normally, montmorillonites are *cv* and illites are *tv*.

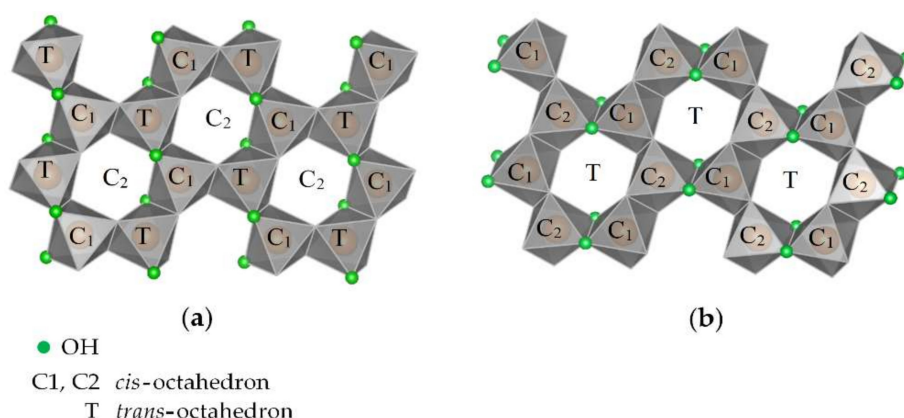


Figure 3. Octahedral sheet of (a) *cis*-vacant configuration and (b) *trans*-vacant configuration in dioctahedral smectites.

In general, 2:1 dioctahedral phyllosilicates show structural defects such as a stacking disorder which makes it difficult to obtain precise structural information by the X-ray powder diffraction (XRD) method, especially for the smectite group [6]. Drits et al. [7] found that the dehydroxylation temperature is related to the structure of the octahedral layer. Since then, the structural transformations have been

extensively studied during dehydroxylation of dioctahedral 2:1 dioctahedral phyllosilicates [8–15]. These studies showed that the chemical composition and the distribution of cations over *cis*- and *trans*-sites in the octahedral sheet are two major factors affecting the dehydroxylation of micas, smectites, and illite/smectite (I/S). The dehydroxylation of *tv* clay minerals occurs in one stage; each two adjacent OH groups form a water molecule and leave one residual oxygen atom, the octahedral cations become five-coordinated. The dehydroxylation of *cv* clay minerals occurs in two stages. First, each two adjacent OH groups are replaced by the residual oxygen atom and the octahedral cations become five- and six-coordinated in *cis*- and *trans*-sites, respectively. Secondly, the cations migrate from *trans*-sites into the former *cis*-vacant site [7,10]. This requires additional thermal energy. Therefore, varieties containing *cv* configuration have dehydroxylation temperature from 100 to 200 °C higher than those consisting of *tv* configuration. The relationships between structural properties and *tv*, *cv* structures has been investigated [16–18]. The octahedral iron content is highly related to the *tv* configuration. The Fe-rich dioctahedral phyllosilicates occur most as a *tv* configuration, and the Al-rich dioctahedral phyllosilicates prefer to form a *cv* configuration [16]. Wolters et al. found that the main influence on the *tv* configuration was due to Fe³⁺ substitution for Al³⁺ in the octahedral sheet [17]. Kaufhold et al. confirmed the relationship between iron content and the ratio of *cv* and *tv* sites from an energy point of view [18]. The dehydroxylation temperature also depended on the iron content.

The information of octahedral structure reflects the thermal reactions which are important for the industrial applications of smectites, for example, the production of supplementary cementitious materials and geopolymers [19]. In addition, the thermal stability of bentonite determines their amount during the foundry process. Therefore, further research about the relationship between the octahedral structure, including *cv* and *tv* varieties, and the physicochemical properties of smectites is necessary in order to gain a better understanding of the formation mechanism of 2:1 dioctahedral phyllosilicates and their industrial application.

The thermal analysis is considered to be an effective method to discriminate the structure of the octahedral sheet. According to Drits et al. [7,8], the *tv* smectites have a dehydroxylation temperature between 500 to 550 °C, and the *cv* smectites have a dehydroxylation temperature about 700 °C. The proportion of the peak areas in different temperatures reflects the proportion of *cis*- and *trans*-vacant configurations. In this study, the thermogravimetric (TG) analysis was used to characterize the structure of the octahedral sheet. The proportions of *cv* and *tv* configurations were calculated by fitting the derivative thermogravimetry (DTG) curves which provided the information of the dehydroxylation reaction, for example, the temperature when water molecules exit the structure from each of the two OH groups. The purpose of this study is to characterize the *tv* and *cv* configurations in dioctahedral smectites by thermogravimetric (TG) analysis and classify samples, to (1) characterize the structure of the octahedral sheet in dioctahedral smectites by thermal analysis and (2) verify the relationships between the proportions of *tv* and *cv* and the structural properties, such as cation distribution in the octahedral and tetrahedral sheets and the layer charge density.

2. Materials and Methods

2.1. Sample Preparation and Characterization

A series of well-investigated dioctahedral smectite samples [17,20] and international reference samples (Source clays, CMS) were used in this study to avoid additional sampling and screening (Table 1). All samples were purified firstly. Only carbonates were found in the bulk samples. The chemical pretreatment to eliminate this impurity was performed according to Tributh and Lagaly [21]. After purification, samples were Na⁺-saturated, and the remaining salt was removed by dialysis. The separation of <0.2 µm fraction was obtained by centrifugation and was applied in order to remove most of impurities, such as quartz [22]. The raw and purified samples were analyzed by XRD. The measurements were performed on an URD 6 instrument using CoK α radiation in 5° to 80° 2 θ range, 0.03° step, and 3 to 5 s/step counting time. An example of one sample before and after purification is

shown in Figure 4. The intensity of reflections of smectite was enhanced significantly after purification. The chemical composition of samples was determined by the X-ray fluorescence analysis (XRF) (Table 2). The measurement was performed on a MagiXPRO XRF-spectrometer. The chemical formula was calculated using the method described by Köster based on one formula unit (FU) $[O_{10}(OH)_2]$ [23]. The layer charge density (LCD) was determined by the alkylammonium method (AAM) [24,25]. The results of chemical formula and the LCD of samples are listed in the studies of Wang et al. [26] and Wang and Liao [27]. The structural information such as octahedral cation content and the LCD obtained by these methods were used to investigate the relationships among the proportions of *cv* and *tv* layers, the cation distribution in octahedral sheet, and the LCD. All the experiments were performed on $<0.2 \mu\text{m}$ fraction. The experimental data of sample characterization originate from studies of Wang et al. [26] and Wang and Liao [27].

Table 1. Origin of samples.

Samples	Description	Source	Supplier
XL_01_B8	Montmorillonite	Wyoming, USA	Bundesanstalt für Geowissenschaften und Rohstoffe (BGR)
XL_02_B9	Montmorillonite	Wyoming, USA	
XL_04_B14	Beidellite	Hungary	
XL_06_B22	Montmorillonite	Hungary	
XL_09_SWy1	Montmorillonite	Wyoming, USA	Society's Source Clays Repository, Clay Minerals Society (CMS)
XL_10_STx1	Montmorillonite	Texas, USA	
XL_11_NAu1	Nontronite	South Australia	
XL_12_NAu2	Nontronite	South Australia	
XL_13_14TR03	Montmorillonite	Unidentified	Karlsruhe Institute of Technology (KIT)
XL_14_41ValC18	Beidellite	Valdagno, Italy	
XL_16_4JUP	Montmorillonite	Argentina	
XL_17_2LP	Montmorillonite	Argentina	
XL_18_Valdol	Beidellite	Valdagno, Italy	
XL_19_NWa	Nontronite	Washington, USA	

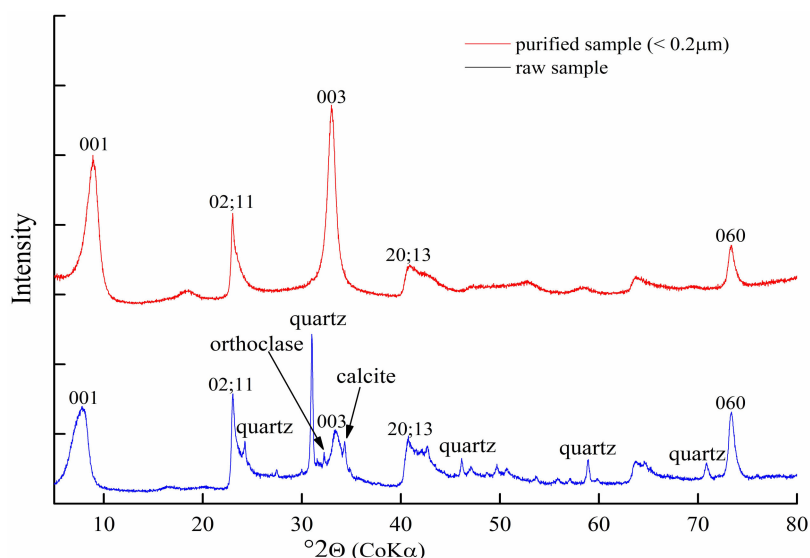


Figure 4. X-ray powder diffraction (XRD) patterns of Sample XL_09_SWy1 before and after purification.

Table 2. Chemical compositions of samples measured by XRF analysis (<0.2 µm fraction).

Samples	Oxides (%)													LOI *	Sum
	SiO ₂	Al ₂ O ₃	Fe ₂ O ₃	MnO	MgO	CaO	K ₂ O	NaO	TiO ₂	CuO	P ₂ O ₅	Cr ₂ O ₃	NiO		
XL_01_B8	55.18	19.98	4.40	0.01	1.74	0.05	0.03	0.00	0.14	3.42	0.00	0.00	0.00	15.05	100.01
XL_02_B9	60.25	17.03	3.74	0.01	2.19	0.03	0.03	0.00	0.12	2.86	0.01	0.00	0.00	13.74	100.00
XL_04_B14	46.63	18.17	11.10	0.02	1.95	0.04	0.50	0.00	2.24	3.01	0.12	0.03	0.02	16.16	100.00
XL_06_B22	59.93	16.24	1.22	0.00	3.53	0.03	0.04	0.00	0.15	3.79	0.00	0.00	0.00	15.07	100.00
XL_09_SWy1	55.19	19.78	4.19	0.01	2.66	0.03	0.03	0.00	0.10	3.12	0.00	0.00	0.00	14.89	100.00
XL_10_STx1	58.03	18.10	2.00	0.01	2.93	0.04	0.06	0.00	0.27	3.16	0.02	0.00	0.00	15.37	100.00
XL_11_NAu1	43.63	7.36	30.25	0.01	0.00	0.03	0.01	0.00	0.03	3.82	0.00	0.01	0.01	14.85	100.00
XL_12_NAu2	48.35	2.49	32.67	0.00	0.01	0.04	0.02	0.00	0.04	3.07	0.00	0.00	0.01	13.30	100.00
XL_13_14TR03	55.14	16.60	1.76	0.01	4.98	0.03	0.02	0.00	0.09	4.09	0.00	0.00	0.00	17.27	100.00
XL_14_41ValC18	52.29	16.06	8.40	0.01	3.65	0.03	0.98	0.00	0.29	3.18	0.04	0.04	0.03	15.00	100.00
XL_16_4JUP	52.29	18.24	7.44	0.03	2.13	0.04	0.32	0.00	0.93	3.11	0.03	0.00	0.00	15.45	100.00
XL_17_2LP	54.20	18.62	4.48	0.02	3.00	0.03	0.06	0.00	0.15	2.99	0.00	0.00	0.00	16.44	100.00
XL_18_Valdol	49.85	15.26	10.44	0.02	3.70	0.05	1.07	0.00	0.39	3.04	0.11	0.04	0.03	16.00	100.00
XL_19_NWa	46.53	8.64	23.02	0.02	1.65	0.02	0.05	0.00	0.60	2.97	0.02	0.01	0.00	16.46	100.00

* LOI: loss on ignition.

2.2. Thermal Analysis

The thermogravimetric (TG) and differential thermal analysis (DTA) measurements were performed on the device SETARAM TGA 92-16.18. Before analysis, samples were stored in a desiccator over a saturated magnesium nitrate solution $\text{Mg}(\text{NO}_3)_2$ (53% RH) for at least 24 h to create a constant humidity condition. Then, a 30 mg sample was used for each measurement, with a heating rate of $10\text{ }^\circ\text{C}/\text{min}$ in the temperature range of 25 to $1000\text{ }^\circ\text{C}$. The proportions of *cis*- and *trans*-vacant configurations were calculated by fitting the derivative thermogravimetry (DTG) curves in the range of 300 to $900\text{ }^\circ\text{C}$ using the PeakFit program v4.12 (2007, Systat Software Inc., San Jose, CA, USA). According to Drits et al. [8], the areas of DTG peaks with the temperature below and above $600\text{ }^\circ\text{C}$ correspond to the amount of *trans*- and *cis*-vacant configurations, respectively, in dioctahedral smectites. Each sample was fitted until the coefficient of determination R^2 was >0.999 . The classification of *cv* and *tv* varieties was based on Wolters and Emmerich [28] (Table 3).

Table 3. Classification of dioctahedral smectites according to the thermal reaction (according to Wolters and Emmerich [28]).

Varieties	<i>cv</i>	<i>cv/tv</i>	<i>tv/cv</i>	<i>tv</i>
the area of dehydroxylation peaks above $600\text{ }^\circ\text{C}/\%$	100–75	74–50	49–25	24–0

3. Results and Discussion

3.1. Characterization and Classification of Octahedral Structure

Figure 5 shows the thermal behavior of samples with mainly *cv* and *tv* configurations. The dehydration of both samples was at around $120\text{ }^\circ\text{C}$. The dehydroxylation temperature of the samples with mainly *cv* structure was around $700\text{ }^\circ\text{C}$ and the sample with mainly *tv* structure was around $500\text{ }^\circ\text{C}$, which agreed well with previous studies [7,8,28,29].

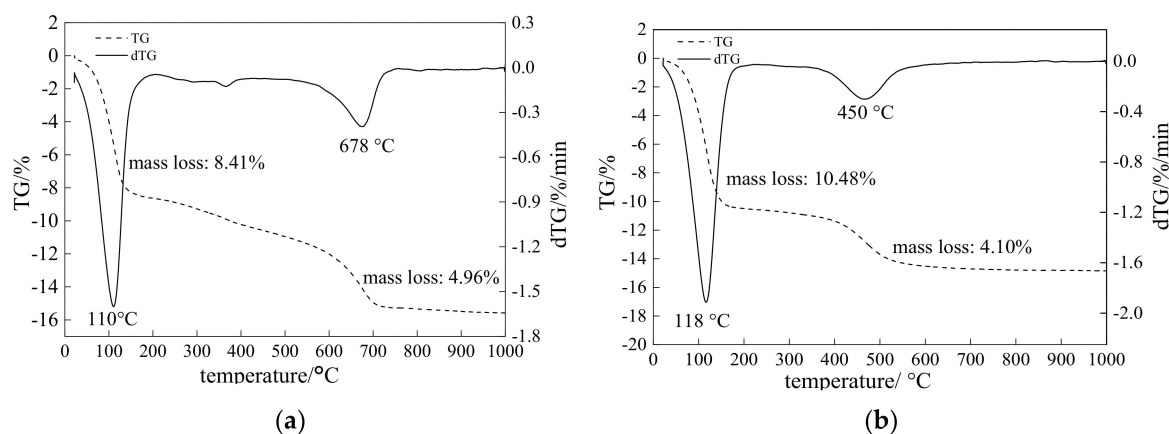
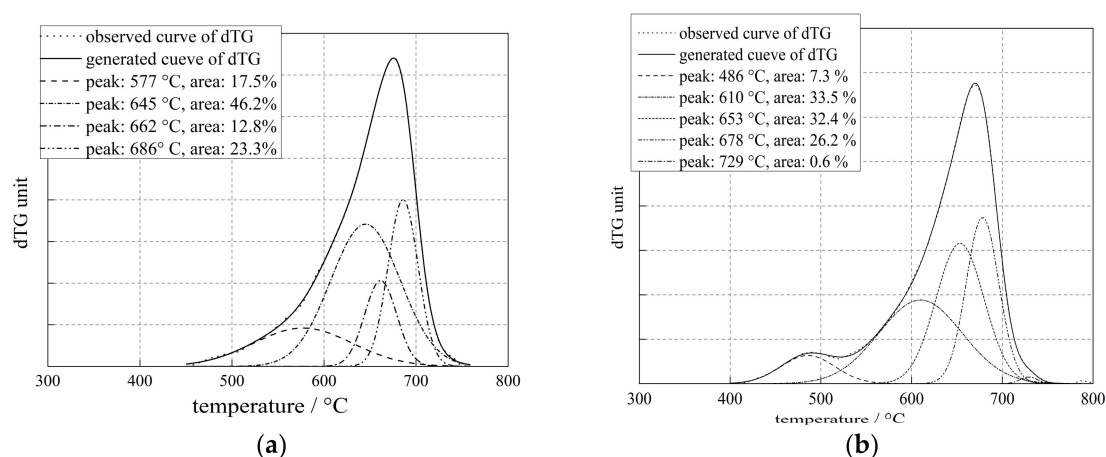


Figure 5. Thermal analysis of (a) sample XL_01_B8 with mainly *cv* structure; (b) Sample XL_12_NAu2 with *tv* structure.

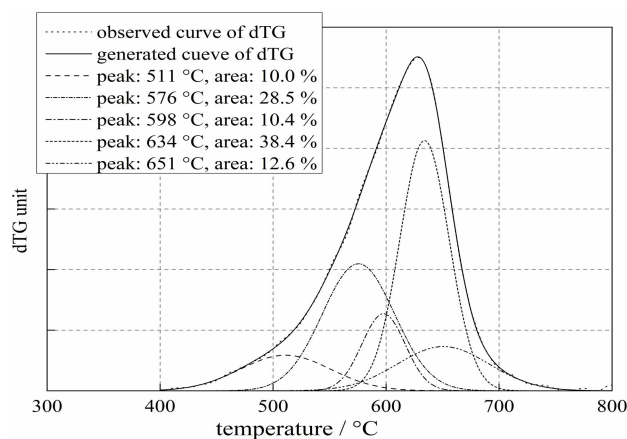
The results of the classification are presented in Table 4. Fourteen samples covered a wide range of *cis*- and *trans*-vacant varieties and the mixtures of them, i.e., *cv*, *cv/tv*, *tv/cv* and *tv* (Table 4). Five samples were considered to be *cv* varieties with a small amount of *tv* configurations (Table 4). Samples XL_06_B22, XL_09_SWy1, and XL_17_2LP showed a similar peak profile with that of sample XL_01_B8, as shown in Figure 6a, and they showed a main peak near $700\text{ }^\circ\text{C}$. Additionally, sample XL_10_STx1 had a small broad peak around $500\text{ }^\circ\text{C}$, which indicated a small amount of *tv* (Figure 6b).

Table 4. The cations content and the proportions of *trans*- (W_{tv}) and *cis*-vacant (W_{cv}) configurations of samples and the classification.

Sample	Tetrahedral Cation (mol/FU)	Octahedral Cations (mol/FU)			Octahedral Sheet		Classification
	Al ³⁺	Al ³⁺	Fe ³⁺	Mg ³⁺	W_{cv} (%)	W_{tv} (%)	
XL_01_B8	0.12	1.58	0.24	0.19	82.5	17.5	<i>cv</i>
XL_06_B22	0.09	1.53	0.08	0.45	90.0	10.0	
XL_09_SWy1	0.12	1.53	0.22	0.28	87.7	12.3	
XL_10_STx1	0.00	1.57	0.11	0.32	92.8	7.2	
XL_17_2LP	0.10	1.48	0.24	0.32	95.7	4.3	
XL_02_B9	0.41	1.55	0.27	0.32	57.0	43.0	<i>cv/tv</i>
XL_13_14TR03	0.00	1.42	0.10	0.54	51.1	48.9	
XL_16_4JUP	0.20	1.40	0.41	0.24	47.6	52.4	<i>tv/cv</i>
XL_04_B14	0.44	1.23	0.65	0.23	1.3	98.7	<i>tv</i>
XL_11_NAu1	0.49	0.21	1.83	0.00	0.0	100.0	
XL_12_NAu2	0.19	0.04	1.94	0.00	0.0	100.0	
XL_14_41ValC18	0.17	1.22	0.47	0.40	15.0	85.0	
XL_18_Valdol	0.25	1.10	0.59	0.42	17.1	82.3	
XL_19_NWa	0.42	0.43	1.46	0.21	0.8	99.2	

**Figure 6.** Examples of derivative thermogravimetry (DTG) curves of *cv* smectites. (a) Sample XL_01_B8 with 82.5% of *cv* layers; (b) Sample XL_10_STx1 with 92.8% of *cv* layers.

Samples XL_02_B9 and XL_13_14TR03 can be classified as *cv/tv* varieties. They had a main peak above 600 °C which indicate one dehydroxylation reaction (Figure 7). Thus, the *cv* configurations dominated in these two samples (Table 4).

**Figure 7.** Examples of derivative thermogravimetry (DTG) curves of *cv/tv* smectites. Sample XL_13_14TR03 with 51.1% *cv* layers and 48.9% *tv* layers.

Sample XL_16_4JUP was *tv/cv* varieties. It contained two well resolved peaks in the *cv* and *tv* region which indicated two main dehydroxylation reactions, i.e., around 490 °C and 650 °C (Figure 8). The sum of the peak area below 600 °C (52.4%) was larger than the area above 600 °C (47.6%), even though the peak at around 630 °C was stronger than the peak at around 490 °C. Therefore, the amount of *tv* is larger than the amount of *cv*. Thus, the *tv* configurations dominated in this sample.

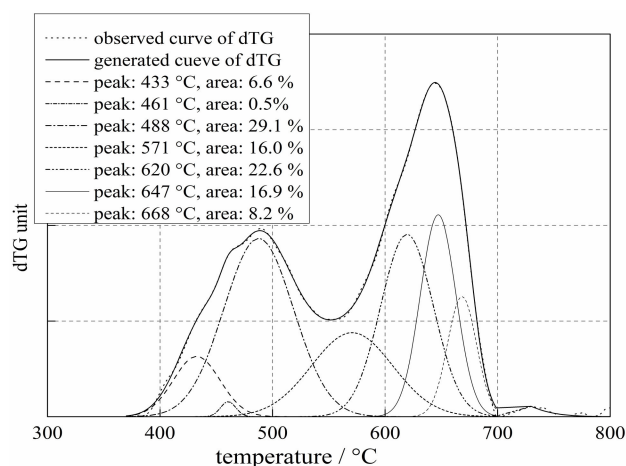


Figure 8. Examples of derivative thermogravimetry (DTG) curves of *tv/cv* smectites. Sample XL_16_4JUP with 52.4% *tv* layers and 47.6% *cv* layers.

Six samples were classified as *tv* varieties (Table 4), i.e., three nontronite samples XL_11_NAu1, XL_12_NAu2 and XL_19_NWa; three beidellite samples XL_04_B14, XL_18_Valdol and XL_14_41ValC18. Tshipursky and Drits [5] showed that montmorillonite and some Al-rich smectites are *cis*-vacant structure, beidellites and nontronites typically have a *trans*-vacant structure. As expected, nontronite samples XL_11_NAu1 and XL_12_NAu2 were found to be purely *trans*-vacant configurations, another nontronite sample XL_19_NWa contained 99.2% *tv* structure. These three nontronites samples show similar dehydroxylation behavior to sample XL_04_B14; they had only one strong peak around 450 °C as shown in Figure 9a. It indicated one dehydroxylation reaction at this temperature. Two resolved peaks were also found in *tv* samples XL_14_41ValC18 and XL_18_Valdol, that showed similar derivative thermogravimetry (DTG) curves with a DTG peak at around 500 °C than the peak at around 630 °C (Figure 9b).

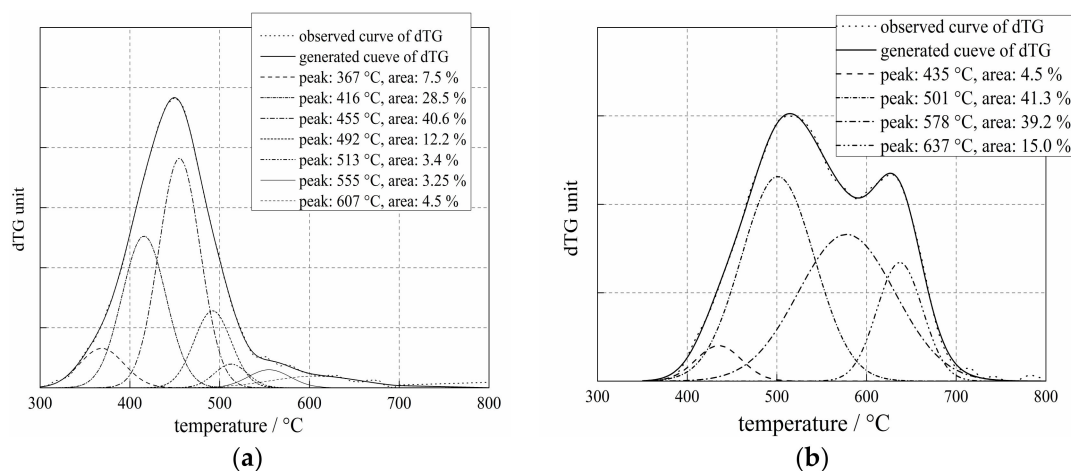


Figure 9. Examples of derivative thermogravimetry (DTG) curves of *tv* smectites. (a) Sample XL_11_NAu1 with 100% of *tv* layers; (b) Sample XL_14_41ValC18 with 85% of *tv* layers.

In summary, five samples were classified as the *cv* variety with the main dehydroxylation reaction near 700 °C and six samples were classified as the *tv* variety with the main dehydroxylation reaction near 500 °C. The remaining three samples contained two well resolved peaks corresponding to two main dehydroxylation reactions between 500 and 700 °C. Two of these samples were considered to be the *cv/tv* type; one of them was considered to be the *tv/cv* type, and the ratio between the peak areas reflected the ratio between *cv* and *tv* layers. The results of the proportions of *cv* and *tv* configurations by thermal analysis agree with the expectations and confirm the classification of the selected samples.

3.2. Relationship between Octahedral Cations and Octahedral Structure

Drits et al. [16] considered that there was a compositional control on the distribution of octahedral cations over *trans*- and *cis* sites in dioctahedral smectites. Therefore, the relationships between the cation distribution in the octahedral sheet and the *cv*, *tv* varieties were investigated. No relationship between the octahedral Mg^{2+} content and the proportion of *tv* and *cv* was detected (Figure 10). It indicated that the octahedral Mg^{2+} content is not correlated to the configuration of the octahedral sheets. In contrast, the influences of octahedral Fe^{3+} and Al^{3+} content on the structure of octahedral sheets is highly significant. A linear relationship was found between octahedral Fe^{3+} and Al^{3+} content and proportion of *cv* and *tv* configurations (Figure 11). The proportion of *tv* structure was increased with increasing octahedral Fe^{3+} content and decreasing octahedral Al^{3+} content. It indicates that the substitution of Al^{3+} by Fe^{3+} in octahedral sheet could be the main reason for the formation of *tv* varieties. Wolters and Emmerich [28] concluded that iron content controls the octahedral structure which is consistent with our study. Samples can be classified as *tv* varieties when octahedral $Fe^{3+} > 0.46$ mol/FU, and pure *tv* varieties were found when octahedral $Fe^{3+} > 1.8$ mol/FU (Table 4, nontronite samples XL_11_NAu1 and XL_12_NAu2). These two nontronites were found with a main dehydroxylation peak in the region around 450 °C (Figures 5b and 9a). It is worth noting that the iron content affects the thermal stability of clay minerals; high iron content can reduce the dehydroxylation temperature due to the differences in bonding energy in the order $Mg-OH > Al-OH > Fe-OH$ [17,30]. This can be one of the reasons that nontronites show a lower dehydroxylation temperature and *tv* configuration.

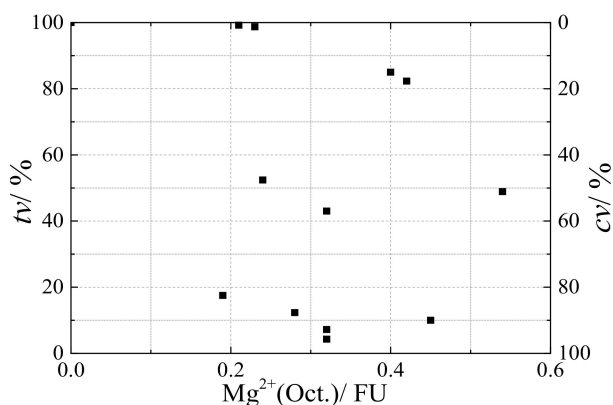


Figure 10. Relationship of the proportion of *tv* and *cv* layers to octahedral Mg^{2+} content.

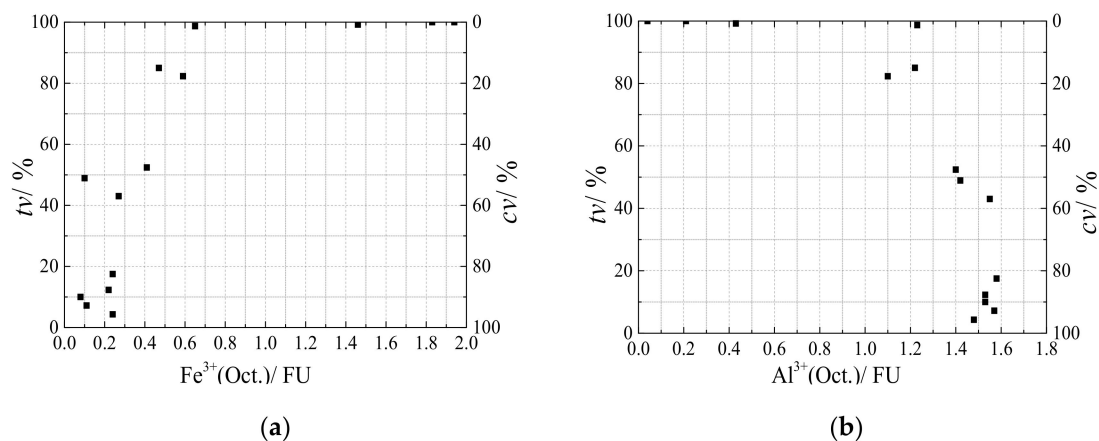


Figure 11. Relationship of the proportion of tv and cv layers to (a) octahedral Fe^{3+} content and (b) octahedral Al^{3+} content.

3.3. Relationship between Layer Charge Density and Octahedral Structure

The present results show that there is no relation between the proportion tv and cv configurations to the total layer charge density (Figure 12a). However, the relationship between the proportion of tv configuration to tetrahedral charge is more significant (Figure 12b). Wolters et al. [17] found a positive correlation between tetrahedral charge and the proportion of tv configuration which is consistent with our results.

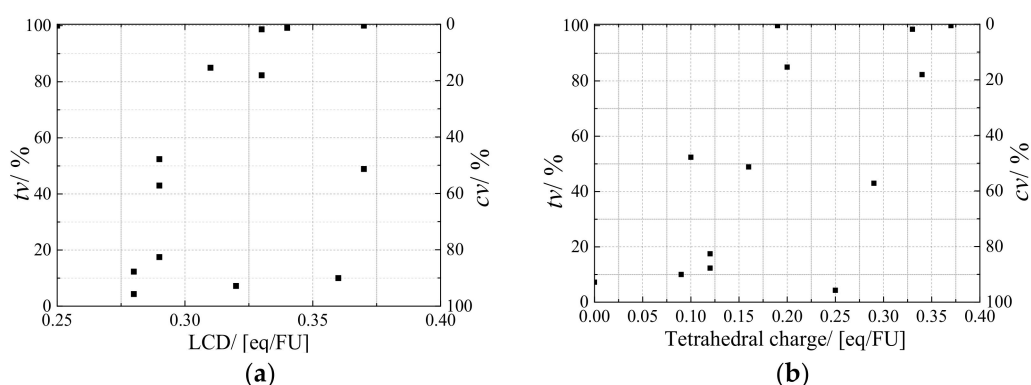


Figure 12. Relationship of the proportion of tv and cv layers to (a) layer charge density (LCD) and (b) tetrahedral charge.

Furthermore, the content of tetrahedral Al^{3+} is positively correlated with octahedral Fe^{3+} content, i.e., the content of tetrahedral Al^{3+} increases with the octahedral Fe^{3+} increasing (Figure 13). Cuadros [31] concluded that this could be because the tetrahedral b dimension is bigger than the octahedral b dimension. He concluded that an increase in octahedral $Mg^{2+} + Fe^{3+}$ causes an increase in tetrahedral Al^{3+} when correlating the ideal b dimension of octahedral and tetrahedral sheets. Cuadros [31] pointed out that the octahedral sheet with cv structure has a smaller b dimension than the tv structure. Therefore, when the tetrahedral sheets have a low substitution (low tetrahedral charge), the sample tends to prefer the cv structure; otherwise, it tends to be the tv structure. Kaufhold et al. confirmed that the existence of a positive correlation between iron content and tetrahedral charge from an energy point of view [18]. The authors concluded that the ratio of tv and cv depends on the iron content which is due to the octahedral iron or tetrahedral Al substitutions [18]. It can be concluded that the iron content is a dominant factor in the positive correlation between the proportion of tv , cv configurations, and the tetrahedral charge. The high iron content is another factor for the lower dehydroxylation temperature of tv configuration than cv configuration.

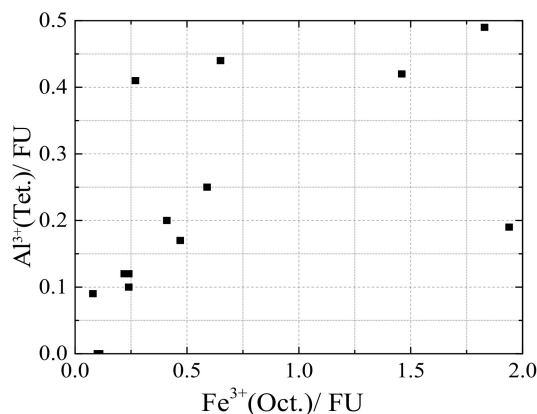


Figure 13. Relationship between tetrahedral Al³⁺ content and octahedral Fe³⁺ content.

4. Conclusions

As expected, the dehydroxylation temperature of samples with mainly *cv* configuration is about 680 °C and for samples with mainly *tv* configuration it is around 500 °C. The proportions of *cv* and *tv* can be determined by fitting the derivative thermogravimetry (DTG) curves. On the one hand, samples which were classified as the *cv* variety showed a main dehydroxylation peak near 680 °C. On the other hand, samples which were classified as the *tv* variety showed a main dehydroxylation peak between 450 and 500 °C. Samples of *cv/tv* and *tv/cv* varieties presented one main peak with a broad shoulder in their own region or two well resolved peaks in the *cv* and *tv* region which indicated two main dehydroxylation reactions. The content of *cv* and *tv* configurations is dependent on the chemical composition. The octahedral Fe³⁺ and Al³⁺ contents were highly related to the proportion of *trans*- and *cis*-vacant structures. With an increasing amount of octahedral Fe³⁺ and a decreasing amount of octahedral Al³⁺, the proportions of the *tv* increased. Pure *tv* dioctahedral smectites were formed when Fe³⁺ > 1.8 mol/FU. No pure *cv* configuration was found in these samples. No relationships among the total layer charge, octahedral Mg²⁺ content, and the proportion *tv* and *cv* were detected. A positive correlation between the tetrahedral charge and *trans*-vacancies was found and the octahedral iron content influences the tetrahedral charge. The present results indicate that the iron content has a significant effect on the structure of the octahedral sheet.

Author Contributions: Conceptualization H.W. and X.W.; data curation X.W.; formal analysis Y.L. and X.W.; writing—initial drafts X.W.; writing—review and editing Y.L., H.W., and X.W. All authors have read and agree to the published version of the manuscript.

Funding: This work was supported by the China Postdoctoral Science Foundation funded project (no. 2019M650320).

Acknowledgments: The authors greatly appreciate Reinhard Kleeberg (TU Bergakademie Freiberg) for his support in the laboratory and valuable comments which improved the manuscript. The authors thank Katja Emmerich and Annett Steudel (Karlsruhe Institute of Technology, KIT) for the assistance in the fitting of DTG curves by the PeakFit program. The authors would like to thank Gerhard Heide (TU Bergakademie Freiberg) for all the support during this work.

Conflicts of Interest: The authors declare no conflict of interest.

References

- Murray, H.H. Bentonite Applications. In *Applied Clay Mineralogy: Occurrences, Processing and Application of Kaolins, Bentonites, Palygorskite-Sepiolite, and Common Clays*, 1st ed.; Elsevier: Amsterdam, The Netherlands, 2007; Volume 2, pp. 111–130.
- Brigatti, M.F.; Galan, E.; Theng, B.K.G. Structures and mineralogy of clay minerals. In *Handbook of Clay Science*, 1st ed.; Bergaya, F., Theng, B.K.G., Lagaly, G., Eds.; Elsevier: Amsterdam, The Netherlands, 2006; Volume 1, pp. 35–43.
- Güven, N. Smectites. In *Hydrous Phyllosilicates*; Bailey, S., Ed.; Mineralogical Society of America: Washington, DC, USA, 1988; Volume 19, pp. 497–559.

4. Méring, J.; Oberlin, A. The Smectites. In *The Electron Optical Investigation of Clays*; Gard, J.A., Ed.; Mineralogical Society: London, UK, 1971; Volume 3, pp. 193–229.
5. Tsipursky, S.I.; Drits, V.A. The distribution of octahedral cations in the 2:1 layers of dioctahedral smectites studied by oblique-texture electron diffraction. *Clay Miner.* **1984**, *19*, 177–193. [[CrossRef](#)]
6. Moore, D.M.; Reynolds, R.C., Jr. *X-ray Diffraction and the Identification and Analysis of Clay Minerals*, 2nd ed.; Oxford University Press: New York, NY, USA, 1997; pp. 335–339.
7. Drits, V.A.; Besson, G.; Muller, F. An improved model for structural transformations of heat-treated aluminous dioctahedral 2:1 layer silicates. *Clays Clay Miner.* **1995**, *43*, 718–731. [[CrossRef](#)]
8. Drits, V.A.; Lindgreen, H.; Salyn, A.L.; Ylagan, R.; McCarty, D.K. Semiquantitative determination of trans-vacant and cis-vacant 2:1 layers in illites and illite-smectites by thermal analysis and X-ray diffraction. *Am. Mineral.* **1998**, *83*, 1188–1198. [[CrossRef](#)]
9. Drits, V.A.; Sakharov, B.A.; Dainyak, L.G.; Salyn, A.L.; Lindgreen, H. Structural and chemical heterogeneity of illite-smectites from Upper Jurassic mudstones of East Greenland related to volcanic and weathered parent rocks. *Am. Mineral.* **2002**, *87*, 1590–1607. [[CrossRef](#)]
10. Drits, V.A.; Zviagina, B.B. Trans-vacant and cis-vacant 2:1 layer silicates: Structural features, identification, and occurrence. *Clays Clay Miner.* **2009**, *57*, 405–415. [[CrossRef](#)]
11. Muller, F.; Drits, V.A.; Plançon, A.; Besson, G. Dehydroxylation of Fe³⁺, Mg-rich dioctahedral micas: (I) Structural transformation. *Clay Miner.* **2000**, *35*, 491–504. [[CrossRef](#)]
12. Muller, F.; Drits, V.A.; Tsipursky, S.I.; Plançon, A. Dehydroxylation of Fe³⁺, Mg-rich dioctahedral micas: (II) Cation migration. *Clay Miner.* **2000**, *35*, 505–514. [[CrossRef](#)]
13. Muller, F.; Drits, V.A.; Plançon, A.; Robert, J.L. Structural transformation of 2:1 dioctahedral layer silicates during dehydroxylation-rehydroxylation reactions. *Clays Clay Miner.* **2000**, *48*, 572–585. [[CrossRef](#)]
14. Dainyak, L.G.; Zviagina, B.B.; Rusakov, V.S.; Drits, V.A. Interpretation of the nontronite dehydroxylate Mössbauer spectrum using EFG calculations. *Eur. J. Miner.* **2006**, *18*, 753–764. [[CrossRef](#)]
15. Marchel, C.; Stanjek, H. Cation ordering in cis- and trans-vacant dioctahedral smectites and its implications for growth mechanisms. *Clay Miner.* **2012**, *47*, 105–115. [[CrossRef](#)]
16. Drits, V.A.; McCarty, D.K.; Zviagina, B.B. Crystalchemical factors responsible for the distribution of octahedral cations over trans- and cis-sites in dioctahedral 2:1 layer silicates. *Clays Clay Miner.* **2006**, *54*, 131–152. [[CrossRef](#)]
17. Wolters, F.; Lagaly, G.; Kahr, G.; Nüesch, R.; Emmerich, K. A comprehensive characterization of dioctahedral smectites. *Clays Clay Miner.* **2009**, *57*, 115–133. [[CrossRef](#)]
18. Kaufhold, S.; Kremleva, A.; Krüger, S.; Roesch, N.; Emmerich, K.; Dohrmann, R. Crystal-chemical composition of dioctahedral smectites: An energy-based assessment of empirical relations. *ACS Earth Space Chem.* **2017**, *1*, 629–636. [[CrossRef](#)]
19. Davidovits, J. Geopolymers: Gerpolymeres and geopolymerische Materialien. *J. Therm. Anal.* **1998**, *35*, 429–441. [[CrossRef](#)]
20. Ufer, K.; Stanjek, H.; Roth, G.; Kleeberg, R.; Dohrmann, R.; Kaufhold, S. Quantitative phase analysis of bentonites by the Rietveld method. *Clays Clay Miner.* **2008**, *56*, 272–282. [[CrossRef](#)]
21. Tributh, H.; Lagaly, G. Aufbereitung und Identifizierung von Boden- und Lagerstättentonen. I. Aufbereitung der Proben im Labor. *GIT-Fachzeitschrift für das Laboratorium* **1986**, *30*, 524–529.
22. Środoń, J. Identification and quantitative analysis of clay minerals. In *Handbook of Clay Science*, 1st ed.; Bergaya, F., Theng, B.K.G., Lagaly, G., Eds.; Elsevier: Amsterdam, The Netherlands, 2006; Volume 1, pp. 765–776.
23. Köster, H.M. Die Berechnung kristallchemischer Strukturformeln von 2:1 Schichtsilikaten unter Berücksichtigung der gemessenen Zwischenschichtladungen und Kationenumtauschkapazitäten, sowie der Darstellung der Ladungsverteilung in der Struktur mittels Dreieckskoordinaten. *Clay Miner.* **1977**, *12*, 45–54. [[CrossRef](#)]
24. Lagaly, G.; Weiss, A. The layer charge of smectitic layer silicates. In *Proceedings of the International Clay Conference, Mexico City, Mexico, 16–23 July 1975*; pp. 157–172.
25. Laird, D.A.; Scott, A.D.; Fenton, T.E. Evaluation of the alkylammonium method of determining layer charge. *Clays Clay Miner.* **1989**, *37*, 41–46. [[CrossRef](#)]
26. Wang, X.L.; Kleeberg, R.; Ufer, K. Routine investigation of important structural parameters of dioctahedral smectites by the Rietveld method. *Appl. Clay Sci.* **2018**, *163*, 257–264. [[CrossRef](#)]

27. Wang, X.L.; Liao, L.B. Rietveld structure refinement of Cu-trien exchanged nontronites. *Front. Chem.* **2018**, *6*, 558. [[CrossRef](#)]
28. Wolters, F.; Emmerich, K. Thermal reactions of smectites-Relation of dehydroxylation temperature to octahedral structure. *Thermochim. Acta* **2007**, *462*, 80–88. [[CrossRef](#)]
29. Emmerich, K.; Kahr, G. The cis- and trans-vacant variety of a montmorillonite: An attempt to create a model smectite. *Appl. Clay Sci.* **2001**, *20*, 119–127. [[CrossRef](#)]
30. Köster, H.M.; Schwertmann, U. Dreischichtminerale. In *Tonminerale und Tone*; Jasmund, K., Lagaly, G., Eds.; Steinkopff Verlag: Darmstadt, Germany, 1993; pp. 33–58.
31. Cuadros, J. Structural insights from the study of Csexchanged smectites submitted to wetting and drying cycles. *Clay Miner.* **2002**, *37*, 473–486. [[CrossRef](#)]



© 2020 by the authors. Licensee MDPI, Basel, Switzerland. This article is an open access article distributed under the terms and conditions of the Creative Commons Attribution (CC BY) license (<http://creativecommons.org/licenses/by/4.0/>).